J Physiol 586.21 (2008) pp 5063–5075

The Journal of Physiology

Comparison of the myoplasmic calcium transient elicited by an action potential in intact fibres of *mdx* and normal mice

Stephen Hollingworth[1], Ulrike Zeiger[1,2] and Stephen M. Baylor[1,2]

[1]*Department of Physiology and* [2]*the Pennsylvania Muscle Institute, University of Pennsylvania School of Medicine, Philadelphia, PA 19104-6085, USA*

The myoplasmic free $[Ca^{2+}]$ transient elicited by an action potential ($\Delta[Ca^{2+}]$) was compared in fast-twitch fibres of *mdx* (dystrophin null) and normal mice. Methods were used that maximized the likelihood that any detected differences apply *in vivo*. Small bundles of fibres were manually dissected from extensor digitorum longus muscles of 7- to 14-week-old mice. One fibre within a bundle was microinjected with furaptra, a low-affinity rapidly responding fluorescent calcium indicator. A fibre was accepted for study if it gave a stable, all-or-nothing fluorescence response to an external shock. In 18 normal fibres, the peak amplitude and the full-duration at half-maximum (FDHM) of $\Delta[Ca^{2+}]$ were 18.4 ± 0.5 μM and 4.9 ± 0.2 ms, respectively (mean ± S.E.M.; 16°C). In 13 *mdx* fibres, the corresponding values were 14.5 ± 0.6 μM and 4.7 ± 0.2 ms. The difference in amplitude is statistically highly significant ($P = 0.0001$; two-tailed *t* test), whereas the difference in FDHM is not ($P = 0.3$). A multi-compartment computer model was used to estimate the amplitude and time course of the sarcoplasmic reticulum (SR) calcium release flux underlying $\Delta[Ca^{2+}]$. Estimates were made based on several differing assumptions: (i) that the resting myoplasmic free Ca^{2+} concentration ($[Ca^{2+}]_R$) and the total concentration of parvalbumin ($[Parv_T]$) are the same in *mdx* and normal fibres, (ii) that $[Ca^{2+}]_R$ is larger in *mdx* fibres, (iii) that $[Parv_T]$ is smaller in *mdx* fibres, and (iv) that $[Ca^{2+}]_R$ is larger and $[Parv_T]$ is smaller in *mdx* fibres. According to the simulations, the 21% smaller amplitude of $\Delta[Ca^{2+}]$ in *mdx* fibres in combination with the unchanged FDHM of $\Delta[Ca^{2+}]$ is consistent with *mdx* fibres having a ∼25% smaller flux amplitude, a 6–23% larger FDHM of the flux, and a 9–20% smaller total amount of released Ca^{2+} than normal fibres. The changes in flux are probably due to a change in the gating of the SR Ca^{2+}-release channels and/or in their single channel flux. The link between these changes and the absence of dystrophin remains to be elucidated.

(Resubmitted 24 July 2008; accepted after revision 1 September 2008; first published online 4 September 2008)
Corresponding author S. M. Baylor: Department of Physiology, University of Pennsylvania School of Medicine, Philadelphia, PA 19104-6085, USA. Email: baylor@mail.med.upenn.edu

Dystrophin is a cytoskeletal protein that links actin filaments to proteins in the plasmalemma. In Duchenne muscular dystrophy (DMD), loss of dystrophin leads to injury and death of skeletal muscle cells. Fast glycolytic fibres (type IIb) show a greater susceptibility to damage than oxidative fibres, at least in the initial stages of DMD (Webster *et al.* 1988; Minetti *et al.* 1991). The primary patho-physiological defect that leads to muscle cell damage is still unresolved, but a widely held view is that dystrophin and its associated proteins protect the fragile plasmalemma from the mechanical stresses that accompany contractile activity (McArdle *et al.* 1995). One long-standing hypothesis (reviewed by Gillis, 1999) is that loss of dystrophin leads to increased Ca^{2+} influx and abnormalities in the myoplasmic free calcium concentration ($[Ca^{2+}]$), and that these abnormalities contribute to the injury and death of muscle cells.

The *mdx* mouse, which lacks dystrophin, is a widely used animal model of DMD. Both the resting myoplasmic free $[Ca^{2+}]$ ($[Ca^{2+}]_R$) and electrically evoked changes in $[Ca^{2+}]$ ($\Delta[Ca^{2+}]$) have been compared in fast-twitch fibres of *mdx* and normal mice, but there are significant qualitative and quantitative disagreements between different studies. $[Ca^{2+}]_R$ in *mdx* fibres has been reported to be normal (Gailly *et al.* 1993; Head, 1993; Pressmar *et al.* 1994; Collet *et al.* 1999; Han *et al.* 2006) and 25–140% above normal (Turner *et al.* 1988, 1991; Hopf *et al.* 1996; Tutdibi *et al.* 1999). In addition, in *mdx* mice > 35 weeks of age, $[Ca^{2+}]_R$ is reported to be 75% below normal (Collet *et al.* 1999). The amplitude of $\Delta[Ca^{2+}]$ evoked by an action potential (AP) has been reported to

DOI: 10.1113/jphysiol.2008.160507

be normal (Turner *et al.* 1988, 1991; Tutdibi *et al.* 1999; see also Head, 1993) and about half normal (Woods *et al.* 2004). The decay time course of the AP-evoked $\Delta[Ca^{2+}]$ has been reported to be normal (Head, 1993), somewhat longer than normal (Turner *et al.* 1988, 1991; Tutdibi *et al.* 1999; see also Collet *et al.* 1999), and markedly longer than normal (Woods *et al.* 2004). Experimental differences that may contribute to these variable findings include the age of the mice, the muscle chosen for experimentation, the method of fibre preparation, the Ca^{2+} indicator used for the measurements, and the method of introducing the indicator into the myoplasm.

Here we compare measurements of $\Delta[Ca^{2+}]$ elicited by an AP in fast-twitch fibres of extensor digitorum longus (EDL) muscles of 7- to 14-week-old *mdx* and normal mice. Our study employed methods that maximize the likelihood that any detected differences apply *in vivo*. These methods included use of: (1) freshly dissected bundles of *intact* fibres (i.e. fibres that are not enzyme-dissociated, dialysed, cut, permeabilized, cultured, or otherwise substantially modified); (2) the Ca^{2+} indicator furaptra (Raju *et al.* 1989), which is a low-affinity, rapidly responding indicator that appears to report accurately the properties of the large and brief $\Delta[Ca^{2+}]$ evoked by an AP in skeletal muscle (Hirota *et al.* 1989; Konishi *et al.* 1991; Hollingworth *et al.* 1996); and (3) microinjection (rather than acetoxymethyl ester (AM)-loading) of furaptra into the fibres, which increases the accuracy of $\Delta[Ca^{2+}]$ measurements (Zhao *et al.* 1997).

A major goal of our study was to see if we could confirm the large reduction in amplitude and large prolongation in time course of $\Delta[Ca^{2+}]$ in *mdx* fibres that was recently reported by Woods *et al.* (2004), who were the first to study $\Delta[Ca^{2+}]$ in *mdx* fibres with a low-affinity Ca^{2+} indicator. Our results indicate that *mdx* fibres have substantially smaller changes in $\Delta[Ca^{2+}]$ than reported by Woods *et al.* (2004). We find that the amplitude of $\Delta[Ca^{2+}]$ elicited by an AP is, on average, 21% smaller in *mdx* than normal fibres while the time course of $\Delta[Ca^{2+}]$ is essentially the same in *mdx* and normal fibres.

We have also used a computational model to estimate the changes in SR Ca^{2+} release flux that are required to explain the changes in $\Delta[Ca^{2+}]$ that we have measured. The results indicate that, in comparison with normal fibres, *mdx* fibres have, on average, a ∼25% smaller peak flux, a 6–23% larger FDHM of the flux, and a 9–20% smaller total amount of released Ca^{2+}.

A preliminary version of the results has appeared in abstract form (Baylor *et al.* 2008).

Methods

Animals

The *mdx* mice were from the C57BL/10ScSn strain lacking dystrophin. The normal mice were from two different strains: C57BL/10 mice, which have the same genetic background as the *mdx* mice, and Balb-C mice. As described in Results, no significant differences were observed between the measurements in the two normal strains. The *mdx* and C57BL/10 mice were a gift of Drs H. L. Sweeney and T. S. Khurana of the University of Pennsylvania. The Balb-C mice were obtained from Charles River Laboratories (Wilmington, MA, USA).

Experimental procedures

Results were collected from experiments on 12 *mdx* mice, 4 C57BL/10 mice, and 8 Balb-C mice, aged 7–14 weeks. Animals were killed by rapid cervical dislocation following methods approved by the Institutional Animal Care and Use Committee of the University of Pennsylvania. The EDL muscles were removed and bathed in an oxygenated Ringer solution containing (in mM): 150 NaCl, 2 KCl, 2 $CaCl_2$, 1 $MgCl_2$, 5 Hepes (pH 7.4). A small bundle of fibres from the most distal head of the EDL muscle was isolated by manual dissection; a group of fibres on the outside edge of the bundle was left undisturbed during dissection (Hollingworth *et al.* 1996). The bundle was transferred to a Ringer-filled chamber (16°C) on an optical bench apparatus, and the tendon ends were attached to adjustable hooks. To minimize movement artifacts in the optical records, the bundle was passively stretched until the average sarcomere length of the fibres was ∼3.6 μm. In a few experiments, the Ringer solution also contained 5 μM BTS (*N*-benzyl-*p*-toluene sulphonamide) to further reduce fibre movement (Cheung *et al.* 2002). One fibre on the undisturbed side of the bundle was impaled with a micropipette containing 15 mM of the permanently charged form of furaptra (K_4Mag-fura-2; Invitrogen, Inc.), which was carefully pressure-injected into the fibre. Indicator fluorescence at rest (F_R) and in response to electrical stimulation (ΔF) was recorded from the full fibre width and a ∼300 μm length near the injection site (furaptra concentration, ∼0.1 mM). The methods for making these spatially averaged measurements have been described (Baylor & Hollingworth, 1988; Konishi *et al.* 1991; Hollingworth *et al.* 1996). In most experiments, the fluorescence excitation and emission wavelengths were 410 ± 20 nm and > 470 nm, respectively. The results are reported in normalized units, $\Delta F/F_R$. A fibre was accepted for study if it gave a stable, all-or-nothing $\Delta F/F_R$ response to an action potential elicited by a brief external shock from a pair of electrodes positioned locally near the injection site.

Fluorescence calibrations

Δf_{CaD}, the spatially averaged change in the fraction of furaptra in the Ca^{2+}-bound form, was calculated from $\Delta F/F_R$. With 410 nm excitation, Δf_{CaD} and $\Delta F/F_R$ are

related by the equation:

$$\Delta f_{CaD} = -1.07\Delta F/F_R \quad (1)$$

(Hollingworth *et al.* 1996; Baylor & Hollingworth, 2003).

Spatially averaged $\Delta[Ca^{2+}]$ was estimated from Δf_{CaD} with the steady-state relation:

$$\Delta[Ca^{2+}] = K_D \Delta f_{CaD}/(1 - \Delta f_{CaD}) \quad (2)$$

(Konishi *et al.* 1991). K_D, furaptra's apparent dissociation constant for Ca^{2+} in the myoplasm, is assumed to be 96 μM (Baylor & Hollingworth, 2003).

Equation (2) assumes that the binding reaction between furaptra and Ca^{2+} is 1 : 1, kinetically rapid, and of low affinity. As discussed previously, $\Delta[Ca^{2+}]$ measured with furaptra is expected to be in approximate agreement with this assumption (Konishi *et al.* 1991). Some error, however, is expected because local elevations in $[Ca^{2+}]$ will be higher near the sites of SR Ca^{2+}-release sites than away from these sites; thus, different regions of the sarcomere will contribute differing non-linearities to the relation between $\Delta[Ca^{2+}]$ and $\Delta F/F_R$ (Baylor & Hollingworth, 2007). The error due to this effect is minimized by use of a low-affinity indicator (Hirota *et al.* 1989; Baylor & Hollingworth, 1998). In simulations of mouse fast-twitch fibres activated by an AP, the estimated error in the amplitude of the furaptra Ca^{2+} transient calculated with eqn (2) is < 10% (Baylor & Hollingworth, 2007).

Estimation of SR Ca^{2+} release

The amplitude and time course of the SR Ca^{2+} release flux underlying $\Delta[Ca^{2+}]$ were estimated with an 18-compartment model that permits simulation of myoplasmic Ca^{2+} movements within a half-sarcomere of one myofibril (Baylor & Hollingworth, 2007; cf. Cannell & Allen, 1984). The SR Ca^{2+} release flux enters the compartment in the model that is at the periphery of the half-sarcomere and offset ~0.5 μm from the z-line, which is the approximate location of the triadic junctions in mammalian fibres (Smith, 1966; Eisenberg, 1983; Brown *et al.* 1998). The resultant changes in free and bound $[Ca^{2+}]$ in the various compartments are then calculated from: (i) $[Ca^{2+}]_R$, (ii) the rate at which Ca^{2+} enters the myoplasm through the SR Ca^{2+} release channels, (iii) the complexation reactions between Ca^{2+} and the major myoplasmic Ca^{2+} buffers (ATP, troponin, parvalbumin, the SR Ca^{2+} pump, and furaptra), (iv) the myoplasmic diffusion of free Ca^{2+} and the mobile Ca^{2+} buffers (ATP, parvalbumin, and furaptra), and (v) the rate at which Ca^{2+} is removed from myoplasm by the SR Ca^{2+} pump. The changes in Ca^{2+} binding and pumping in each compartment and the diffusion of Ca^{2+} and of the mobile Ca^{2+} buffers between compartments are calculated with an appropriate set of first-order differential equations. The parameters of the model for the standard simulation conditions are given in Tables 1–3 of Baylor & Hollingworth (2007). For the *mdx* simulations, no change was made in the complexation reaction between Ca^{2+} and the troponin regulatory sites, as tension–pCa measurements in skinned fibres of EDL muscle indicate that the apparent sensitivity of the contractile proteins to Ca^{2+} is not significantly different in *mdx* and normal fibres (22–25°C, 17- to 23-week-old mice, Williams *et al.* 1993; 22°C, 11-week-old mice, Divet & Huchet-Cadiou, 2002). Some reports in the literature, however, indicate that $[Ca^{2+}]_R$ is higher, and the concentration of parvalbumin is lower, in *mdx* fibres than in normal fibres (see Results). Simulations for *mdx* fibres were therefore carried out with both normal and elevated values of $[Ca^{2+}]_R$ and with both normal and reduced values of the concentration of parvalbumin.

To compare the simulations with the measurements, furaptra's simulated spatially averaged Δf_{CaD} waveform was calculated from the Δf_{CaD} waveforms in the 18 compartments (Baylor & Hollingworth, 2007). Equation (2) was then used to calculate the simulated spatially averaged $\Delta[Ca^{2+}]$ waveform from the spatially averaged Δf_{CaD}. The SR Ca^{2+} release flux was calculated with an empirical function:

$$\text{Release}(t) = R[1 - \exp(-(t - T)/\tau_1)]^5 \exp(-(t - T)/\tau_2)$$

for $t \geq T$. τ_1 was set to 1.3 ms, and T (the delay between the stimulus pulse and the onset of Ca^{2+} release) was set to 1.4 ms. R and τ_2 were adjusted iteratively until good agreement was observed between the peak and FDHM of the simulated $\Delta[Ca^{2+}]$ waveform and the corresponding mean values in the measurements. τ_2 fell in the range 0.5–0.7 ms, which yielded FDHM values of the release flux of 1.6–1.9 ms.

Statistics

Student's two-tailed t test was used to test for differences between mean values; the significance level was set at $P < 0.05$. The parameters tested included the four properties of $\Delta[Ca^{2+}]$ listed in Table 1 and the vertical location of the data points relative to the simulated curve in Fig. 4*A*. For the latter test, points above the curve were assigned the value +1 and those below the curve were assigned −1.

Results

Figure 1 shows results from two representative experiments in which a fibre injected with furaptra was stimulated by an AP (panel *A*, normal fibre; panel *B*, *mdx* fibre). In each panel, the upper trace shows $\Delta F/F_R$

Table 1. Parameters of $\Delta[Ca^{2+}]$ elicited by an action potential in intact EDL fibres (16°C)

	Peak amplitude (μM)	Time of half-rise (ms)	Time of peak (ms)	FDHM (ms)
A. Normal fibres				
1. Balb-C mice ($n = 13$)	18.4 ± 0.5	3.1 ± 0.1	4.4 ± 0.1	4.9 ± 0.2
2. C57BL/10 mice ($n = 5$)	18.5 ± 1.8	3.2 ± 0.3	4.5 ± 0.3	4.9 ± 0.4
3. 1 and 2 combined ($n = 18$)	18.4 ± 0.6	3.2 ± 0.1	4.4 ± 0.1	4.9 ± 0.2
B. *mdx* fibres ($n = 13$)	14.5 ± 0.6*	3.1 ± 0.1	4.3 ± 0.2	4.7 ± 0.2

Entries are mean ± S.E.M. values of $\Delta[Ca^{2+}]$ measured in a total of 31 experiments like those in Fig. 1. None of the parameter values is statistically significantly different between the two strains of normal mice ($P > 0.05$; see also open symbols in Fig. 4). * indicates that the difference in peak amplitudes between *mdx* fibres and all normal fibres (row 3) is statistically significant ($P = 0.0001$); for the other 3 parameters, differences between *mdx* and normal fibres are not significant ($P > 0.05$). The average sarcomere length in the experiments was 3.7 ± 0.1 μm in normal fibres and 3.5 ± 0.1 μm in *mdx* fibres. Some results from the Balb-C mice were reported previously (Hollingworth *et al.* 1996).

and the lower trace shows spatially averaged $\Delta[Ca^{2+}]$, which was calculated from $\Delta F/F_R$ with eqns (1) and (2). The peak of $\Delta[Ca^{2+}]$ is smaller in the *mdx* fibre than in the normal fibre (14.5 *versus* 18.7 μM), whereas the time of half-rise (3.1 *versus* 2.9 ms), time of peak (4.0 *versus* 4.0 ms), and FDHM (4.0 *versus* 4.0 ms) of $\Delta[Ca^{2+}]$ are essentially identical in the two fibres.

Table 1 lists the average properties of $\Delta[Ca^{2+}]$ measured in 18 normal fibres and 13 *mdx* fibres. Results in normal fibres showed no significant differences according to strain (Balb-C *versus* C57BL/10; rows 1 and 2 of Table 1). Peak $\Delta[Ca^{2+}]$ in the *mdx* fibres is, however, 21% smaller than that in the normal fibres (14.5 *versus* 18.4 μM, respectively; rows 3 and 4 of Table 1), a difference that is statistically highly significant ($P = 0.0001$). In contrast, none of the temporal parameters of $\Delta[Ca^{2+}]$ – time of half-rise, time of peak, and FDHM – are statistically different in *mdx* and normal fibres ($P > 0.05$).

SR Ca^{2+} release estimated with the standard parameter values of the model

If $[Ca^{2+}]_R$ and the concentrations of the myoplasmic Ca^{2+} buffers are similar in *mdx* and normal fibres, the

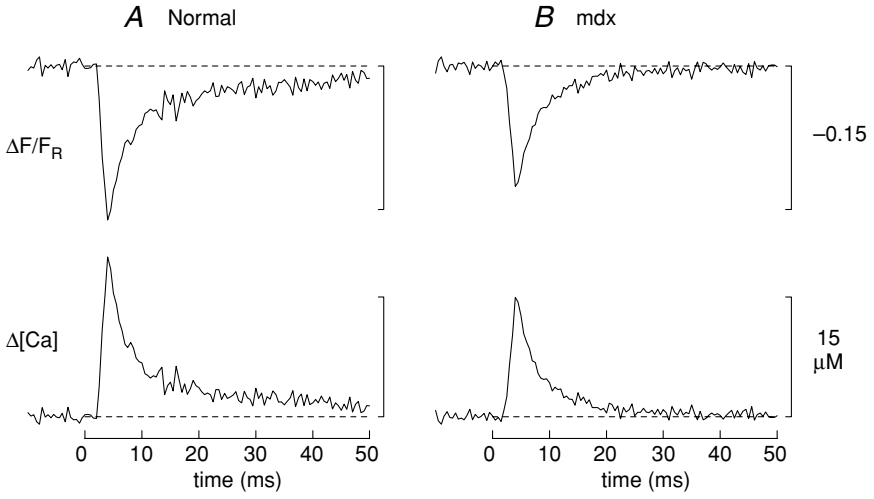

Figure 1. Spatially averaged Ca^{2+} transients elicited by an AP in EDL fibres from C57BL/10 mice
A, normal fibre; *B*, *mdx* fibre. In each panel, the upper trace shows the furaptra $\Delta F/F_R$ response elicited by a supra-threshold external shock initiated at 0 time. The fluorescence excitation and emission wavelengths were 410 ± 20 nm and > 470 nm, respectively; F_R was corrected for a small non-furaptra-related component of intensity. Six individual responses were averaged in *A* and four in *B*; the waiting time between successive shocks was 3 min. In *A*, the Ringer soultion contained 5 μM BTS; thus, this trace is likely to be virtually free of movement artifacts. In *B*, BTS was not used; thus this trace may be contaminated with a small movement artifact beginning 10–15 ms after stimulation. The lower panels show $\Delta[Ca^{2+}]$ calculated from $\Delta F/F_R$ with eqns (1) and (2). Fibre diameters, 42 μm and 39 μm; sarcomere length, 3.8 μm and 3.5 μm; furaptra concentration, 30 and 85 μM.

most likely explanation of the smaller amplitude Ca^{2+} transient in *mdx* fibres is a reduction in the underlying SR Ca^{2+} release flux. To quantify this reduction, simulations were carried out with the 18-compartment model using the standard values of the model parameters (Baylor & Hollingworth, 2007). As described in Methods, in each simulation the amplitude and FDHM of the release flux were adjusted so that the peak and FDHM of the simulated $\Delta[Ca^{2+}]$ waveform matched the corresponding values in Table 1. Figure 2*A* shows the results of these simulations (continuous traces, normal; dashed traces, *mdx*). The SR Ca^{2+} release flux (upper pair of traces) has a peak amplitude that is 26% smaller in the *mdx* simulation (156 *versus* 211 μM ms^{-1}) and a FDHM that is 23% larger (1.93 *versus* 1.57 ms). The net effect of these differences on the change in the total concentration of released Ca^{2+} ($\Delta[Ca_{Total}]$; middle pair of traces) is a 9% reduction in the *mdx* simulation (328 *versus* 359 μM). The lower pair of traces shows the simulated spatially averaged $\Delta[Ca^{2+}]$ waveforms. The results of these simulations are summarized as cases A and B1 in Table 2.

The $\Delta[Ca^{2+}]$ traces in Fig. 2*A* are also shown in panels *B* and *C* of Fig. 2 (noise-free traces; normal and *mdx*, respectively). These traces are also compared with experimental measurements of $\Delta[Ca^{2+}]$, which were averaged from four normal fibres (Fig. 2*B*) and from four *mdx* fibres (Fig. 2*C*); these fibres were selected because their $\Delta F/F_R$ recordings appeared to have little or no contamination with movement artifacts. The good agreement between the simulated and measured traces in Fig. 2*B* and *C* supports the conclusion that the multi-compartment model provides a good description of the intracellular Ca^{2+} movements that underlie the $\Delta[Ca^{2+}]$ measurements.

Estimation of SR Ca^{2+} release if $[Ca^{2+}]_R$ is elevated in *mdx* fibres

Contrary to the assumption in the simulations of Fig. 2*A*, it is possible that myoplasmic properties differ in *mdx* and normal fibres. For example, some studies have reported that $[Ca^{2+}]_R$ is elevated by 25–140% in *mdx* fibres (Turner

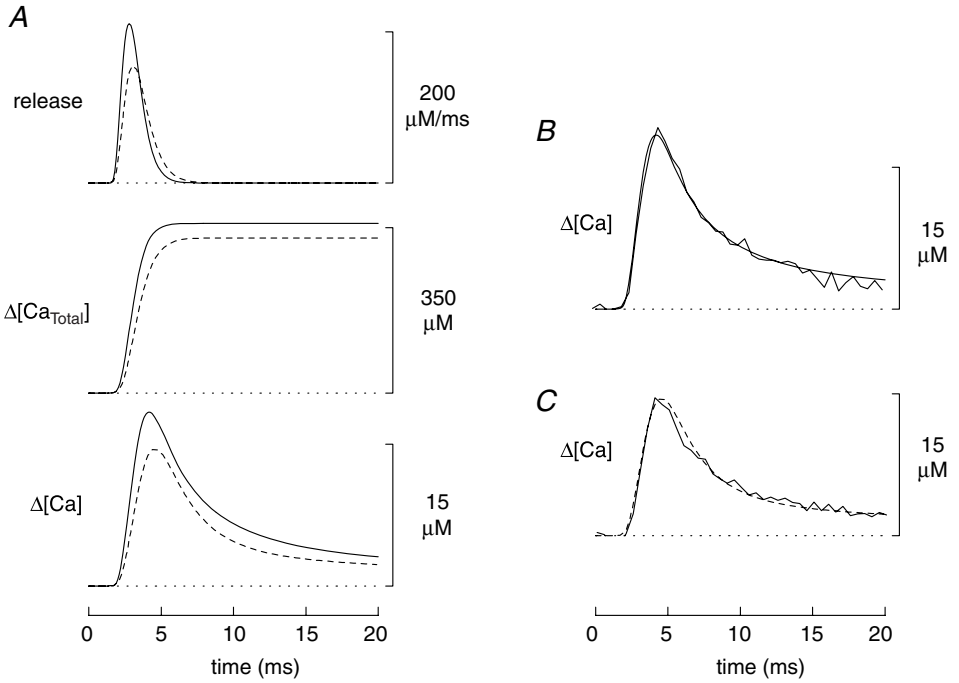

Figure 2
A, comparison of model simulations for normal and *mdx* fibres (continuous and dashed traces, respectively). In both simulations, the standard parameter values of the model were used. The upper, middle and lower traces show, respectively, the SR Ca^{2+} release flux, the change in the total concentration of released Ca^{2+} (equal to the time integral of the flux), and the spatially averaged $\Delta[Ca^{2+}]$ calculated with eqn (2) from the simulated Δf_{CaD} response of furaptra; the concentration units of all traces are referred to the myoplasmic water volume (Baylor *et al.* 1983). The peak and FDHM of the $\Delta[Ca^{2+}]$ traces match the corresponding mean values in the last two rows of Table 1. *B*, comparison of simulated and measured $\Delta[Ca^{2+}]$ waveforms in normal fibres. The simulated waveform (noise-free trace) is identical to the lowermost continuous trace in *A*; the measured waveform (noisy trace) is $\Delta[Ca^{2+}]$ averaged from four normal fibres. *C*, same comparison as in *B* but for *mdx* fibres. The dashed waveform is identical to the lowermost dashed trace in *A*; the continuous waveform was averaged from four *mdx* fibres.

Table 2. Estimation of SR Ca^{2+} release elicited by an action potential in intact EDL fibres (16°C)

	Peak release flux (μM ms^{-1})	FDHM of release flux (ms)	$\Delta[Ca_{Total}]$ (μM)
A. Normal fibres	211	1.57	359
B. *mdx* fibres			
1. With standard model parameters	156 (0.74)	1.93 (1.23)	328 (0.91)
2. With $[Ca^{2+}]_R$ increased 100%	157 (0.74)	1.81 (1.15)	311 (0.87)
3. With $[Parv_T]$ reduced 40%	158 (0.75)	1.75 (1.11)	299 (0.83)
4. With $[Ca^{2+}]_R$ increased 100% and$[Parv_T]$ reduced 40%	158 (0.75)	1.67 (1.06)	288 (0.80)

Entries were obtained from simulations with the multi-compartment model described in Methods (cf. Figs 2 and 3); all concentrations are referred to the myoplasmic water volume. Results for normal fibres and for case 1 of *mdx* fibres used the standard parameter values of the model (Baylor & Hollingworth, 2007). Case 2 of *mdx* fibres used $[Ca^{2+}]_R = 100$ (rather than 50) nM, case 3 used $[Parv_T] = 900$ (rather than 1500) μM, and case 4 used $[Ca^{2+}]_R = 100$ nM and $[Parv_T] = 900$ μM. In all simulations, the amplitude and FDHM of the release flux were adjusted so that the amplitude and FDHM of the simulated $\Delta[Ca^{2+}]$ matched the values in rows 3 and 4 of Table 1 (normal and *mdx*, respectively). In B, the numbers in parentheses give the ratio of the *mdx* value to the corresponding normal value.

et al. 1988, 1991; Hopf *et al.* 1996; Tutdibi *et al.* 1999). To examine this possibility, simulations for *mdx* fibres were carried out with $[Ca^{2+}]_R$ increased by 100%, from its standard value of 50 nM (as in Fig. 2) to 100 nM. The dashed traces in Fig. 3*A* show the result. In this case, the peak of the Ca^{2+} release flux in the *mdx* simulation is 26% smaller than normal (157 *versus* 211 μM ms^{-1}), the FDHM of the release flux is 15% larger (1.81 *versus* 1.57 ms), and $\Delta[Ca_{Total}]$ is 13% smaller (311 *versus* 359 μM) (case B2 in Table 2).

Estimation of SR Ca^{2+} release if $[Parv_T]$ is reduced in *mdx* fibres

Sano *et al.* (1990) reported that, in tibialis anterior muscle (a predominantly fast-twitch muscle), the parvalbumin

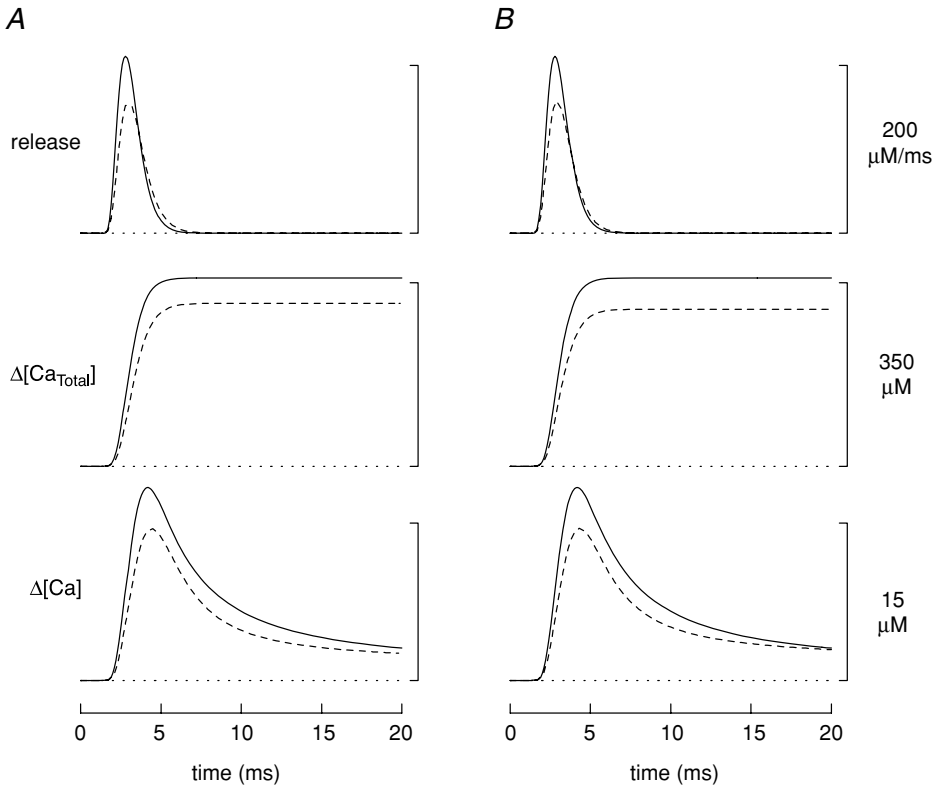

Figure 3
Same comparisons as those in Fig. 2*A* except that, in the *mdx* simulation, $[Ca^{2+}]_R$ is assumed to be 100 (rather than 50) nM (*A*) or $[Parv_T]$ is assumed to be 900 (rather than 1500) μM (*B*).

concentration of 7- to 14-week-old mice is ∼40% smaller in *mdx* fibres than in normal fibres. To examine this possibility, simulations for *mdx* fibres were carried out with $[Parv_T]$ (the concentration of the parvalbumin Ca^{2+}/Mg^{2+} sites in the model) reduced by 40%, from 1500 to 900 μM. The dashed traces in Fig. 3*B* show the result. In this case, the peak of the SR Ca^{2+} release flux is 25% smaller in the *mdx* simulation (158 *versus* 211 μM ms^{-1}), the FDHM of the flux is 11% larger (1.75 *versus* 1.57 ms), and $\Delta[Ca_{Total}]$ is 17% smaller (299 *versus* 359 μM) (case B3 in Table 2).

Estimations of SR Ca^{2+} release if there is both elevation of $[Ca^{2+}]_R$ and reduction of $[Parv_T]$ in *mdx* fibres

Simulations for *mdx* fibres were also carried out with $[Ca^{2+}]_R = 100$ nM and $[Parv_T] = 900$ μM, i.e. the combination of the two previous cases (traces not shown). In this case, the peak of the SR Ca^{2+} release flux is 25% smaller in the *mdx* simulation (158 *versus* 211 μM ms^{-1}), the FDHM of the flux is 6% larger (1.67 *versus* 1.57 ms), and $\Delta[Ca_{Total}]$ is 20% smaller (288 *versus* 359 μM) (case B4 in Table 2).

Relations between the amplitude and FDHM of $\Delta[Ca^{2+}]$

Previous work indicates that, in normal EDL fibres, a positive correlation exists between the FDHM and peak amplitude of $\Delta[Ca^{2+}]$ (Baylor & Hollingworth, 2007). Figure 4 explores this correlation for both normal and *mdx* fibres. Figure 4*A* shows the FDHM of $\Delta[Ca^{2+}]$ plotted *versus* the peak of $\Delta[Ca^{2+}]$ for the 31 fibres used for this study (open symbols, normal fibres; +, *mdx* fibres).

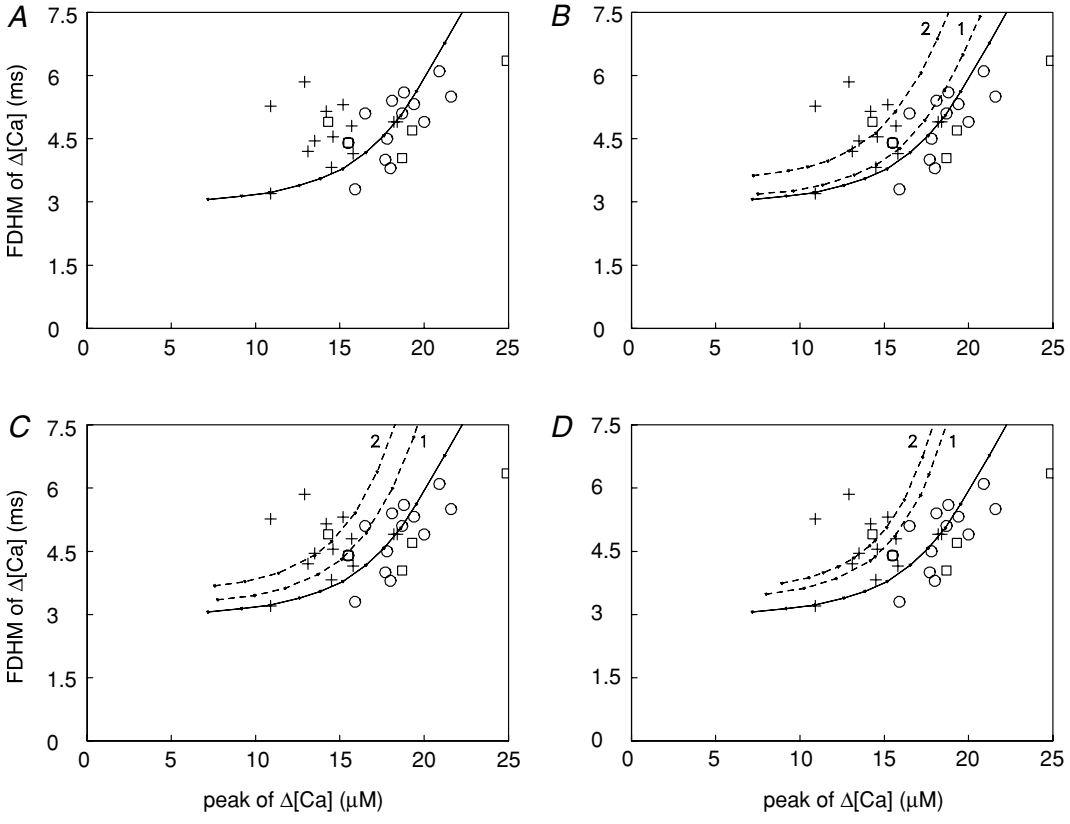

Figure 4. Relations between the FDHM and peak of $\Delta[Ca^{2+}]$ elicited by an AP
A, + represent *mdx* fibres and open symbols represent normal fibres (squares, C57BL/10 mice; circles, Balb-C mice). The continuous curve was obtained in simulations with the standard parameter values of the multi-compartment model; the amplitude of the SR Ca^{2+} release flux was varied incrementally while the FDHM of the flux was fixed at 1.57 ms (the value used for the normal fibre simulation in Table 2). The symbols and curve are also shown in *B–D*. *B*, the dashed curve labelled '1' was obtained in the same way as the continuous curve except that $[Ca^{2+}]_R$ was 100 (rather than 50) nM. Dashed curve '2' was obtained with the same conditions as for curve '1' except that the FDHM of the release flux was 1.81 ms (as in row B2 in Table 2) rather than 1.57 ms. *C* and *D*, dashed curves labelled '1' were obtained as in *B* except that, in *C*, $[Parv_T]$ was 900 (rather than 1500) μM and, in *D*, $[Ca^{2+}]_R$ was 100 nM and $[Parv_T]$ was 900 μM. Dashed curves '2' were obtained with the same conditions as for curves '1' except the FDHM of the release flux was 1.75 ms in *C* and 1.67 ms in *D* (as in rows B3 and B4, respectively, in Table 2).

The data for the normal fibres appear to be positively correlated. As shown by the continuous curve in Fig. 4*A*, such a correlation is expected if the FDHM of the SR release flux is constant and the amplitude of the release flux varies somewhat among otherwise identical fibres. The *mdx* data do not reveal a positive correlation, possibly due to the smaller size of this data set. Interestingly, the relation between amplitude and FDHM in the *mdx* data differs statistically from that in the normal data ($P = 0.003$), as most of the *mdx* data points lie above the curve in Fig. 4*A*, whereas a majority of the normal data points lie below the curve.

The dashed curves in Fig. 4*B–D* explore the idea that the upward shift in the *mdx* data in Fig. 4*A* is a consequence of an increase in $[Ca^{2+}]_R$ and/or a reduction in $[Parv_T]$. Results are shown, respectively, for the cases considered earlier, namely, that (i) $[Ca^{2+}]_R$ is increased, (ii) $[Parv_T]$ is reduced, or (iii) both $[Ca^{2+}]_R$ is increased and $[Parv_T]$ is reduced. In each panel, the relation between amplitude and FDHM of $\Delta[Ca^{2+}]$ in *mdx* fibres was simulated in two ways: either the FDHM of the release flux was kept the same as that used for the continuous curve (dashed curve '1') or the FDHM of the release flux was set to the value in Table 2 for the corresponding case (dashed curve '2'; cf. Figs 2 and 3). In all cases, the dashed curves are shifted upward with respect to the continuous curve and provide a better fit to the *mdx* data than the continuous curve. Thus, the upward shift in the *mdx* data relative to the normal data in Fig. 4 is consistent with the idea that *mdx* fibres have an increase in $[Ca^{2+}]_R$, a reduction in $[Parv_T]$, or both.

Estimation of Ca^{2+} binding to troponin

Model estimates of Ca^{2+} binding to the troponin regulatory sites (two per troponin molecule) were also obtained in the simulations. The complexation reaction between Ca^{2+} and the regulatory sites is assumed to be a two-step reaction with positive cooperativity (Hollingworth *et al.* 2006); the free $[Ca^{2+}]$ at which 50% of the sites are occupied with Ca^{2+} in the steady state is 1.3 μM. In the normal fibre simulation, 0.9% of the troponin sites are occupied with Ca^{2+} at rest and, in response to an AP, the (spatially averaged) peak occupancy reaches 96.3%. In the *mdx* simulations, the resting occupancy is 0.9 and 2.3% ($[Ca^{2+}]_R = 50$ and 100 nM, respectively) and the peak occupancy varies between 90.9 and 92.0% for the four cases summarized in part B of Table 2. Thus, in the *mdx* simulations, the Ca^{2+}-troponin occupancy is reduced only slightly (~5%) as a result of the 21% reduction in the amplitude of $\Delta[Ca^{2+}]$. This small reduction in Ca^{2+}-troponin occupancy might account for part of the reduction in twitch-specific force that is reported for EDL muscle in young adult *mdx* mice: ~10% in 6- to 8-week-old mice (whole muscles at 22–24°C, Chan *et al.* 2007) and 33% in 12-week-old mice (small fibre bundles at 19–22°C, Louboutin *et al.* 1995). On the other hand, a more important factor underlying the reduction in twitch-specific force may reside in the force-generating capability of the myofilaments, as tension–pCa measurements on small bundles of chemically skinned EDL fibres indicate that specific force at saturating $[Ca^{2+}]$ is reduced by ~35% in *mdx* fibres (bundles of 2–5 fibres from 11-week-old mice, 22°C; Divet & Huchet-Cadiou, 2002; see also Williams *et al.* 1993; who reported a ~20% reduction at 22–25°C in chemically skinned single EDL fibres from 17- to 23-week-old mice, a difference that was not statistically significant).

Discussion

This article compares $\Delta[Ca^{2+}]$ elicited by an AP in intact skeletal muscle fibres of *mdx* and normal mice. Measurements were made in fibres injected with the permanently charged form of furaptra, a low-affinity, rapidly responding Ca^{2+} indicator. The preparation and methodology were chosen to maximize the accuracy of the measurements and the likelihood that the results apply *in vivo*.

The measurements show an average reduction of ~20% in the amplitude of $\Delta[Ca^{2+}]$ in *mdx* compared to normal fibres. In contrast, the time of half-rise, time of peak, and FDHM of $\Delta[Ca^{2+}]$ are unchanged in *mdx* fibres (Table 1). It should be noted that the later falling phase of the furaptra ΔF signal (e.g. for time > 15 ms after stimulation; cf. Fig. 1) includes a small component caused by a change in myoplasmic free $[Mg^{2+}]$ (Konishi *et al.* 1991) and, in some experiments, is also contaminated with a movement artifact; thus our measurements do not rule out the possibility that the late falling phase of $\Delta[Ca^{2+}]$ might differ somewhat in *mdx* and normal fibres.

Comparisons with previous $\Delta[Ca^{2+}]$ measurements in *mdx* and normal fibres

Our findings of relatively small differences in $\Delta[Ca^{2+}]$ elicited by an AP in *mdx* and normal fibres differ substantially from those of Woods *et al.* (2004), who compared $\Delta[Ca^{2+}]$ in enzyme-dissociated fibres using the permanently charged form of the low-affinity Ca^{2+} indicator Oregon Green 488 Bapta-5N (OGB-5N). These authors studied fibres from 8- to 18-week-old mice at a sarcomere length of ~2 μm (22°C). Movements artifacts at the short sarcomere length were eliminated either by the introduction of 5 mM EGTA into the myoplasm or by the use of 50 μM BTS. The EGTA experiments, which were carried out in fibres dissociated from both EDL and flexor digitorum brevis (FDB) muscles, are not

directly comparable to ours because 5 mM EGTA modifies $\Delta[Ca^{2+}]$, reducing its amplitude and abbreviating its time course to approximately that of the SR Ca^{2+} release flux (Song *et al.* 1998; Woods *et al.* 2004). The experiments using BTS to reduce movement, which are more comparable to ours, were carried out on fibres dissociated from FDB muscles. In these fibres Woods *et al.* reported that the peak amplitude of $\Delta[Ca^{2+}]$ is reduced by ∼45%, from 6.0 ± 0.1 μM in normal fibres to 3.3 ± 0.2 μM in *mdx* fibres. This reduction in amplitude in *mdx* fibres is more than twice the reduction found by us (21%; Table 1), a difference that appears to be statistically highly significant as judged from the S.E.M.s of amplitude reductions in the two studies (± 3% if expressed as a percentage of the mean amplitude of $\Delta[Ca^{2+}]$ in normal fibres). Woods *et al.* also reported that the FDHM of $\Delta[Ca^{2+}]$ is increased 6-fold in fibres not containing EGTA, from 8 ms in normal fibres to 48 ms in *mdx* fibres. Their value of 48 ms for the FDHM at 22°C stands in marked contrast to our finding that the FDHM in *mdx* fibres is ∼5 ms at 16°C and unchanged from that in normal fibres. In their EGTA experiments, Woods *et al.* (2004) also found that *mdx* fibres have a large reduction in the amplitude of $\Delta[Ca^{2+}]$ elicited by an AP: by 46% in FDB fibres and by 54% in EDL fibres. As expected, the FDHM of $\Delta[Ca^{2+}]$ in these EGTA experiments was brief in all cases, 2–4 ms, due to the Ca^{2+}-buffering action of EGTA.

The reason(s) for the difference between our results on EDL fibres and those of Woods *et al.* (2004) on FDB fibres not containing EGTA is unclear. There is no reason to expect that the properties of $\Delta[Ca^{2+}]$ would differ substantially between fast-twitch fibres of EDL and FDB muscles. In agreement with this expectation, in the EGTA experiments of Woods *et al.* (2004), the properties of $\Delta[Ca^{2+}]$ differed in minor ways only between EDL and FDB fibres from either normal or *mdx* muscles. Thus, it seems unlikely that the differences between our study and that of Woods *et al.* are due to the different muscles employed.

Other experimental differences between our study and that of Woods *et al.* (2004) include the choice of Ca^{2+} indicator (furaptra *versus* OGB-5N, respectively), the method of fibre preparation (intact *versus* enzymatically dissociated), the sarcomere length of the fibres (∼3.6 *versus* ∼2.0 μm), and the method of introducing the indicator into the fibre (pressure injection *versus* passive loading from a low-resistance micropipette in the case of their FDB fibres or passive diffusion from a cut end in the case of their EDL fibres). The fact that different Ca^{2+} indicators were used in the two studies could be significant. OGB-5N is a visible wavelength tetracarboxylate Ca^{2+} indicator of relatively large molecular weight (920 Da for the hexavalent anion); in contrast, furaptra is a shorter wavelength tricarboxylate indicator of smaller molecular weight (430 Da for the tetravalent anion). In general, larger visible wavelength indicators (e.g. calcium orange, calcium-orange-5N, calcium-green-5N, and BTC) bind more heavily to myoplasmic constituents than does furaptra and track the kinetics of $\Delta[Ca^{2+}]$ less reliably (Zhao *et al.* 1996, 1997). In addition, some visible wavelength indicators reveal a prominent slow component that is not directly related to Ca^{2+} complexation (Zhao *et al.* 1996; see also Baylor *et al.* 1982). Thus, it would not be surprising if OGB-5N tracks $\Delta[Ca^{2+}]$ less reliably than furaptra.

Our use of stretched fibres and pressure injection of indicator is also potentially significant, as the absence of dystrophin may increase the fragility of the surface membrane (reviewed in McArdle *et al.* 1995), which could make *mdx* fibres more susceptible to damage by stretch and/or pressure injection. We cannot rule out the possibility that an effect of this kind could contribute to the reduction in the amplitude of $\Delta[Ca^{2+}]$ that we have measured in *mdx* fibres (Table 1). However, the changes in $\Delta[Ca^{2+}]$ in *mdx* fibres found by Woods *et al.* (2004) are much larger than those found by us; thus, the differences between the two studies cannot be attributed to selective membrane damage of our *mdx* fibres by stretch or pressure injection

The isolation of fibres by enzymatic dissociation is clearly more perturbing than isolation of a bundle of intact fibres by careful manual dissection. As noted by Woods *et al.* (2004), immediately following their enzyme dissociations, only a small percentage of fibres actively twitched in response to electrical stimulation; this percentage increased to ∼25% after a 30 min incubation in an O_2-saturated L-15 media (Sigma) containing antibiotics. Although Woods *et al.* experimented only on fibres capable of giving a vigorous twitch, it nevertheless seems possible that the enzyme digestion perturbed the properties of these fibres and produced the large differences between the *mdx* and normal fibres. Against this possibility, however, are results from three other studies in which enzyme digestion was used yet relatively small differences between $\Delta[Ca^{2+}]$ in *mdx* and normal fibres were found. These studies used a high-affinity slowly responding tetra-carboxylate Ca^{2+} indicator – either fura-2 (Head, 1993; Tutdibi *et al.* 1999) or indo-1 (Collet *et al.* 1999); because of this, the ability to accurately distinguish changes in the amplitude and the time course of $\Delta[Ca^{2+}]$ was compromised. Head (1993) found that, in *mdx* fibres, the amplitude of $\Delta[Ca^{2+}]$ elicited by an AP fell within the same 3-fold range found in normal fibres and had the same variability; in addition, the kinetics of $\Delta[Ca^{2+}]$ was indistinguishable in *mdx* and normal fibres out to ∼500 ms after stimulation (22°C). Tutdibi *et al.* (1999), who stimulated fibres repetitively (1 Hz, 20–24°C) rather than with a single AP, found no difference in the amplitude of $\Delta[Ca^{2+}]$ in *mdx* and normal fibres; in contrast, they reported that the decay

time constant of $\Delta[Ca^{2+}]$ in *mdx* fibres, while within the same range as that found for normal fibres (10–55 ms), was, on average, somewhat larger (50% of *mdx* fibres had time constants > 35 ms compared with 20% of normal fibres). In the experiments of Collet *et al.* (1999), who used the voltage-clamp technique to elicit $\Delta[Ca^{2+}]$ with depolarizations from -80 to 0 mV for periods of 5–50 ms (20–22°C), the most notable differences were that *mdx* fibres had a ∼2-fold larger time constant of decay of $\Delta[Ca^{2+}]$ in response to a 5 ms depolarization and a somewhat larger peak $\Delta[Ca^{2+}]$ and final level of $\Delta[Ca^{2+}]$ in response to a 15 ms depolarization. Relatively small differences between $\Delta[Ca^{2+}]$ in *mdx* and normal fibres were also found by Turner *et al.* (1988, 1991), who used intact (rather than enzymatically dissociated) FDB fibres that were AM-loaded with fura-2 and activated by repetitive stimulation (25 and 37°C). These authors found no difference in the amplitude of $\Delta[Ca^{2+}]$ in *mdx* fibres, although they did find an increase in the time to peak of 15–30% and an increase in the decay time constant of 40–60%. Overall, none of these studies that used a high-affinity Ca^{2+} indicator detected a significant reduction in the amplitude of $\Delta[Ca^{2+}]$ in *mdx* fibres. In contrast, Woods *et al.* (2004), who used the high-affinity indicator OGB-1 in some experiments, found that the amplitude of $\Delta[Ca^{2+}]$ was 36% smaller in *mdx* fibres than in normal fibres, which is slightly smaller than the reductions that they found with OGB-5N (45, 46 and 54%, depending on experimental conditions; see above). On balance, the large differences found by Woods *et al.* (2004) in comparison with these other studies and our own suggest that these large differences do not apply to fibres in their normal physiological state. A factor unique to the experiments of Woods *et al.* (2004) is that the myoplasm of their fibres was dialysed with an artificial internal solution (primarily, potassium aspartate) for a period of 30 min prior to optical recording, with recording and dialysis usually continuing for another 30 min or more. This prolonged dialysis procedure might have produced some change in the physiological properties of their fibres (cf. Irving *et al.* 1987), including an increase in the FDHM of $\Delta[Ca^{2+}]$ (Maylie *et al.* 1987).

A final factor that might have contributed to the larger values of the FDHM of $\Delta[Ca^{2+}]$ in the fibres of Woods *et al.* (2004) that did not contain EGTA is the large concentration of BTS, 50 μM, that was used to reduce movement artifacts in the fluorescence measurements. This concentration of BTS prolongs the decay phase of the AP somewhat (Woods *et al.* 2004), which, in turn, would be expected to prolong the time course of SR Ca^{2+} release and of $\Delta[Ca^{2+}]$. In our experiments, we relied primarily on stretch to reduce movement artifacts, although 5 μM BTS was also used in a few experiments (e.g. Fig. 1*A*). In frog twitch fibres, 5 μM BTS does not alter $\Delta[Ca^{2+}]$ and is not expected to alter the AP (Cheung *et al.* 2002).

In summary, we believe that the relatively small differences that we have detected between $\Delta[Ca^{2+}]$ in *mdx* and normal EDL fibres probably represent the main changes that apply *in vivo* to fast-twitch fibres of 7- to 14-week-old mice. The exact reason for the much larger effects detected in the experiments of Woods *et al.* (2004) remains unclear.

Evidence that myoplasmic properties are different in *mdx* and normal fibres

In our experiments, the observed values of the FDHM of $\Delta[Ca^{2+}]$ in *mdx* fibres are larger than expected based on the measured reductions in the peak amplitude of $\Delta[Ca^{2+}]$ in *mdx* fibres and on the relation between the FDHM and peak of $\Delta[Ca^{2+}]$ observed in normal fibres (Fig. 4*A*). The larger-than-expected FDHM values in *mdx* fibres are consistent with the idea that *mdx* fibres have an increase in $[Ca^{2+}]_R$ (Turner *et al.* 1988, 1991; Hopf *et al.* 1996; Tutdibi *et al.* 1999), a reduction in the concentration of parvalbumin (Sano *et al.* 1990), or both (Fig. 4*B–D*). The effect of an increase in $[Ca^{2+}]_R$ is similar to that of a reduction in $[Parv_T]$ because the main effect of an increase in $[Ca^{2+}]_R$ is to reduce the availability of metal-free sites on parvalbumin. These sites bind Ca^{2+} rapidly and contribute to the early decay of $\Delta[Ca^{2+}]$ (Baylor & Hollingworth, 2007); consequently, a reduction in these sites leads to a larger FDHM of $\Delta[Ca^{2+}]$ for a given amplitude of $\Delta[Ca^{2+}]$.

In Fig. 4, there appears to be a greater scatter in the *mdx* data than in the normal data. A possible explanation for this effect is that *mdx* fibres have a greater percentage variation in $[Ca^{2+}]_R$ and/or $[Parv_T]$ than normal fibres. Another factor that may possibly contribute is some minor damage in the *mdx* fibres due to our use of long sarcomere length and/or pressure injection of indicator (see above).

Differences between SR Ca^{2+} release in *mdx* and normal fibres

Our compartment modelling indicates that the properties of $\Delta[Ca^{2+}]$ elicited by an AP in *mdx* fibres are consistent with these fibres having, on average, a ∼25% smaller peak SR Ca^{2+} release flux, a 6–23% larger FDHM of the flux, and a 9–20% smaller total amount of released Ca^{2+} than normal fibres (Table 2). Some increase in the FDHM of the release flux would be expected to accompany a reduction in the amplitude of $\Delta[Ca^{2+}]$, as previous work indicates that $\Delta[Ca^{2+}]$ feeds back rapidly in a negative fashion to inhibit release (Baylor *et al.* 1983; Schneider & Simon, 1988; Baylor & Hollingworth, 1988; Jong *et al.* 1995). Thus, if the amplitude of $\Delta[Ca^{2+}]$ is smaller, the effectiveness of the feedback inhibition should be reduced,

and a prolongation of the time course of the release flux would be expected.

Woods *et al.* (2004, 2005) also compared the peak rate of SR Ca^{2+} release in *mdx* and normal fibres. In contrast to our results, they estimated larger reductions in release in *mdx* fibres – by 46% in response to a single AP and by 67% in response to a voltage-clamp depolarization to 0 mV. These large reductions are related to the large reductions in the amplitude of $\Delta[Ca^{2+}]$ measured with OGB-5N in their *mdx* fibres (Woods *et al.* 2004, 2005; see also the second section of Discussion). As discussed above, the precise reason for the large effects detected by Woods *et al.* remains to be elucidated.

Possible mechanisms underlying a reduction in SR Ca^{2+} release in *mdx* fibres

Previous reports indicate that a number of key determinants of the excitation–contraction coupling process in skeletal muscle are similar in *mdx* and normal fibres, including the resting membrane potential (Hollingworth *et al.* 1990; Mathes *et al.* 1991), the action potential (Woods *et al.* 2004), the structure and electrical charging of the transverse tubules (Woods *et al.* 2005), and the amount and kinetics of voltage-dependent charge movement (Hollingworth *et al.* 1990; Collet *et al.* 2003). If these similarities also apply under the experimental conditions of our study, the most likely explanation for the reduction in SR Ca^{2+} release that we estimate occurs in *mdx* fibres is a change either in the gating of the SR Ca^{2+}-release channels (ryanodine receptors, RyRs) or in their single channel Ca^{2+} flux. Possible contributing factors include alteration(s) in the myoplasmic constituents, the constituents within the lumen of the SR, and/or the proteins of the SR membrane, including the RyRs and the SR Ca^{2+} pump. Such alterations might be caused by a chronic elevation of $[Ca^{2+}]_R$ (Turner *et al.* 1988, 1991; Hopf *et al.* 1996; Tutdibi *et al.* 1999), which is often associated with a reduction in electrically evoked SR Ca^{2+} release (Lamb *et al.* 1995; Chin & Allen, 1996; Yeung *et al.* 2005). A chronic elevation of $[Ca^{2+}]_R$ could result in increased activity of proteases such as calpains (e.g. Turner *et al.* 1988; Gillis, 1999; Gailly *et al.* 2007), which could alter the normal structural arrangement between the t-tubular and SR membranes (Verburg *et al.* 2005) and hence the physiological coupling between the t-tubular voltage sensors and the RyRs. An increase in $[Ca^{2+}]_R$ could also compromise the metabolic state of the fibre (e.g. Dunn *et al.* 1991; Whitehead *et al.* 2006), which could inhibit gating of RyRs by altering the concentrations of key myoplasmic constituents such as ATP, ADP, Mg^{2+} and H^+. In addition, *mdx* fibres are reported to have a reduction in the activity of the SR Ca^{2+} pump (Kometani *et al.* 1990; Kargacin & Kargacin, 1996; Divet & Huchet-Cadiou, 2002) and a reduction in Ca^{2+}-binding proteins within the SR (Culligan *et al.* 2002; Dowling *et al.* 2004; Doran *et al.* 2004). This could result in a reduced SR Ca^{2+} load, a reduced driving force for Ca^{2+} release, and a reduced single channel Ca^{2+} flux.

References

Baylor SM, Chandler WK & Marshall MW (1982). Dichroic components of arsenazo III and dichlorophosphonazo III signals in skeletal muscle fibres. *J Physiol* **331**, 179–210.

Baylor SM, Chandler WK & Marshall MW (1983). Sarcoplasmic reticulum calcium release in frog skeletal muscle fibres estimated from arsenazo III calcium transients. *J Physiol* **344**, 625–666.

Baylor SM & Hollingworth S (1988). Fura-2 calcium transients in frog skeletal muscle fibres. *J Physiol* **403**, 151–192.

Baylor SM & Hollingworth S (1998). Model of sarcomeric Ca^{2+} movements, including ATP Ca^{2+} binding and diffusion, during activation of frog skeletal muscle. *J Gen Physiol* **112**, 297–316.

Baylor SM & Hollingworth S (2003). Sarcoplasmic reticulum calcium release compared in slow-twitch and fast-twitch fibres of mouse muscle. *J Physiol* **551**, 125–138.

Baylor SM & Hollingworth S (2007). Simulation of Ca^{2+} movements within the sarcomere of fast-twitch mouse fibres stimulated by action potentials. *J Gen Physiol* **130**, 283–302.

Baylor SM, Zeiger U & Hollingworth S (2008). Comparison of the spatially-averaged myoplasmic calcium transient (Δ[Ca]) elicited by an action potential (AP) in fast-twitch fibers of normal and *mdx* mice. Biophysical Society Meeting Abstract. *Biophys J* **94**, 308a.

Brown IE, Kim DH & Loeb GE (1998). The effect of sarcomere length on triad location in intact feline caudofemoralis muscle fibres. *J Muscle Res Cell Motil* **19**, 473–477.

Cannell MB & Allen DG (1984). Model of calcium movements during activation in the sarcomere of frog skeletal muscle. *Biophys J* **45**, 913–925.

Chan S, Head SI & Morley JW (2007). Branched fibres in dystrophic *mdx* muscle are associated with a loss of force following lengthening contractions. *Am J Physiol Cell Physiol* **93**, C985–C992.

Cheung A, Dantzig JA, Hollingworth S, Baylor SM, Goldman YE, Mitchison TJ & Straight AF (2002). A small-molecule inhibitor of skeletal muscle myosin II. *Nature Cell Biol* **4**, 83–88.

Chin ER & Allen DG (1996). The role of elevations in intracellular Ca^{2+} concentration in the development of low frequency fatigue in mouse single muscle fibres. *J Physiol* **491**, 813–824.

Collet C, Allard B, Tourneur Y & Jacquemond V (1999). Cellular calcium signals measured with indo-1 in isolated skeletal muscle fibres from control and *mdx* mice. *J Physiol* **520**, 417–429.

Collet C, Csernoch L & Jacquemond V (2003). Intramembrane charge movement and L-type calcium current in skeletal muscle fibres from control and *mdx* mice. *Biophys J* **84**, 251–265.

Culligan K, Banville N, Dowling P & Ohlendieck K (2002). Drastic reduction of calsequestrin-like proteins and impaired calcium binding in dystrophic *mdx* muscle. *J Appl Physiol* **92**, 435–445.

Divet A & Huchet-Cadiou C (2002). Sarcoplasmic reticulum function in slow- and fast-twitch skeletal muscles from mdx mice. *Pflugers Arch* **444**, 634–643.

Doran P, Dowling P, Lohan J, McDonnell K, Poetsch S & Ohlendieck K (2004). Subproteomics analysis of Ca^{2+}-binding proteins demonstrates decreased calsequestrin expression in dystrophic mouse skeletal muscle. *Eur J Biochem* **271**, 3943–3952.

Dowling P, Doran P & Ohlendieck K (2004). Drastic reduction of sarcalumenin in Dp427 (dystrophin of 427 kDa)-deficient fibres indicates that abnormal calcium handling plays a key role in muscular dystrophy. *Biochem J* **379**, 479–488.

Dunn JF, Frostick S, Brown G & Radda GK (1991). Energy status of cells lacking dystrophin: an in vivo/in vitro study of *mdx* mouse skeletal muscle. *Biochim Biophys Acta* **1096**, 115–120.

Eisenberg BR (1983). Quantitative ultrastructure of mammalian skeletal muscle. In *Handbook of Physiology*, section 10, *Skeletal Muscle*, ed. Peachey LD, Adrian RH & Geiger SR, pp. 73–112. Williams & Wilkins, Baltimore.

Gailly P, Boland B, Himpens B, Casteels R & Gillis JM (1993). Critical evaluation of cytosolic calcium determination in resting muscle fibres from normal and dystrophic (mdx) mice. *Cell Calcium* **14**, 473–483.

Gailly P, De Backer F, Van Schoor M & Gillis JM (2007). *In situ* measurements of calpain activity in isolated muscle fibres from normal and dystrophin-lacking *mdx* mice. *J Physiol* **582**, 1261–1275.

Gillis JM (1999). Understanding dystrophinopathies: an inventory of the structural and functional consequences of the absence of dystrophin in muscles of the *mdx* mouse. *J Mus Res Cell Motility* **20**, 605–625.

Han R, Grounds MD & Bakker AJ (2006). Measurement of sub-membrane $[Ca^{2+}]$ in adult myofibres and cytosolic $[Ca^{2+}]$ in myotubes from normal and *mdx* mice using the Ca^{2+} indicator FFP-18. *Cell Calcium* **40**, 299–307.

Head SI (1993). Membrane potential, resting calcium and calcium transients in isolated muscle fibres from normal and dystrophic mice. *J Physiol* **469**, 11–19.

Hirota A, Chandler WK, Southwick PL & Waggoner AS (1989). Calcium signals recorded from two new purpurate indicators inside frog cut twitch fibres. *J Gen Physiol* **94**, 597–631.

Hollingworth S, Chandler WK & Baylor SM (2006). Effects of tetracaine on calcium sparks in frog intact skeletal muscle fibres. *J Gen Physiol* **127**, 291–307.

Hollingworth S, Marshall MW & Robson E (1990). Excitation contraction coupling in normal and mdx mice. *Muscle Nerve* **13**, 16–20.

Hollingworth S, Zhao M & Baylor SM (1996). The amplitude and time course of the myoplasmic free $[Ca^{2+}]$ transient in fast-twitch fibres of mouse muscle. *J Gen Physiol* **108**, 455–469.

Hopf FW, Turner PR, Denetclaw WF, Reddy R & Steinhardt RA (1996). A critical evaluation of resting intracellular free calcium regulation in dystrophic *mdx* muscle. *Am J Physiol Cell Physiol* **271**, C1325–C1339.

Irving M, Maylie J, Sizto NL & Chandler WK (1987). Intrinsic optical and passive electrical properties of cut frog twitch fibres. *J Gen Physiol* **89**, 1–40.

Jong D-S, Pape PC, Baylor SM & Chandler WK (1995). Calcium inactivation of calcium release in frog cut muscle fibres that contain millimolar EGTA or Fura-2. *J Gen Physiol* **106**, 337–388.

Kargacin ME & Kargacin GJ (1996). The sarcoplasmic reticulum calcium pump is functionally altered in dystrophic muscles. *Biochim Biophys Acta* **1290**, 4–8.

Kometani K, Tsugeno H & Yamada K (1990). Mechanical and energetic properties of dystrophic (*mdx*) mouse muscle. *Jap J Physiol* **40**, 541–549.

Konishi M, Hollingworth S, Harkins AB & Baylor SM (1991). Myoplasmic calcium transients in intact frog skeletal muscle fibres monitored with the fluorescent indicator furaptra. *J Gen Physiol* **97**, 271–301.

Lamb GD, Junankar PR & Stephenson DG (1995). Raised intracellular $[Ca^{2+}]$ abolishes excitation-contraction coupling in skeletal muscle fibres of rat and toad. *J Physiol* **489**, 349–362.

Louboutin JP, Fichter-Gagnepain V, Pastoret C, Thaon E, Noireaud J, Sebille A & Fardeau M (1995). Morphological and functional study of extensor digitorum longus muscle regeneration after iterative crush lesions in *mdx* mouse. *Neuromuscul Disord* **5**, 489–500.

McArdle A, Edwards RHT & Jackson MJ (1995). How does dystrophin deficiency lead to muscle degeneration? – Evidence from the *mdx* mouse. *Neuromuscul Disord* **5**, 445–456.

Mathes C, Bezanilla F & Weiss RE (1991). Sodium current and membrane potential in EDL muscle fibres from normal and dystrophic (*mdx*) mice. *Am J Physiol Cell Physiol* **261**, C718–C725.

Maylie J, Irving M, Sizto NL & Chandler WK (1987). Comparison of arsenazo III optical signals in intact and cut frog twitch fibres. *J Gen Physiol* **89**, 41–81.

Minetti C, Ricci E & Bonilla E (1991). Progressive depletion of fast alpha-actinin-positive muscle fibres in Duchenne muscular dystrophy. *Neurology* **41**, 1977–1981.

Pressmar J, Brinkmeier H, Seewald MJ, Naumann T & Rudel R (1994). Intracellular Ca^{2+} concentrations are not elevated in resting cultured muscle from Duchenne (DMD) patients and in MDX mouse muscle fibres. *Pflugers Arch* **426**, 499–505.

Raju B, Murphy E, Levy LA, Hall RD & London RE (1989). A fluorescent indicator for measuring cytosolic free magnesium. *Am J Physiol Cell Physiol* **256**, C540–C548.

Sano M, Yokota T, Endo T & Tsukagoshi H (1990). A developmental change in the content of parvalbumin in normal and dystrophic mouse (mdx) muscle. *J Neurol Sci* **97**, 261–272.

Schneider MF & Simon BJ (1988). Inactivation of calcium release from the sarcoplasmic reticulum in frog skeletal muscle. *J Physiol* **405**, 727–745.

Smith DS (1966). The organization and function of the sarcoplasmic reticulum and T system of muscle cells. *Prog Biophys Mol Biol* **16**, 109–142.

Song L-S, Sham JSK, Stern MD, Lakatta EG & Cheng H (1998). Direct measurement of SR release flux by tracking 'Ca spikes' in rat cardiac myocytes. *J Physiol* **512**, 677–691.

Turner PR, Fong PY, Denetclaw WF & Steinhardt RA (1991). Increased calcium influx in dystrophic muscle. *J Cell Biol* **115**, 1701–1712.

Turner PR, Westwood T, Regen CM & Steinhardt RA (1988). Increased protein degradation results from elevated free calcium levels found in muscle from *mdx* mice. *Nature* **335**, 735–738.

Tutdibi O, Brinkmeier H, Rudel R & Fohr KJ (1999). Increased calcium entry into dystrophin-deficient muscle fibres of MDX and ADR-MDX mice is reduced by ion channel blockers. *J Physiol* **515**, 859–898.

Verburg E, Murphy RM, Stephenson DG & Lamb GD (2005). Disruption of excitation-contraction coupling and titin by endogenous Ca^{2+}-activated proteases in toad muscle fibres. *J Physiol* **564**, 775–789.

Webster C, Silberstein L, Hays AP & Blau HM (1988). Fast muscle fibres are preferentially affected in Duchenne muscular dystrophy. *Cell* **52**, 503–513.

Whitehead NP, Yeung EW & Allen DG (2006). Muscle damage in *mdx* (dystrophic) mice: role of calcium and reactive oxygen species. *Clin Exp Pharmacol Physiol* **33**, 657–662.

Williams DA, Head SI, Lynch GS & Stephenson DG (1993). Contractile properties of skinned muscle fibres from young and adult normal and dystrophic (*mdx*) mice. *J Physiol* **460**, 51–67.

Woods CE, Novo D, DiFranco M, Capote J & Vergara JL (2005). Propagation in the transverse tubular system and voltage dependence of calcium release in normal and *mdx* mouse muscle fibres. *J Physiol* **568**, 867–880.

Woods CE, Novo D, DiFranco M & Vergara JL (2004). The action potential-evoked sarcoplasmic reticulum calcium release is impaired in *mdx* mouse muscle fibres. *J Physiol* **557**, 59–75.

Yeung EW, Whitehead NP, Suchyna TM, Gottlieb PA, Sachs F & Allen DG (2005). Effects of stretch-activated channel blockers on $[Ca^{2+}]_i$ and muscle damage in the *mdx* mouse. *J Physiol* **562**, 367–380.

Zhao M, Hollingworth S & Baylor SM (1996). Properties of tri- and tetra-carboxylate Ca^{2+} indicators in frog skeletal muscle fibres. *Biophys J* **70**, 896–916.

Zhao M, Hollingworth S & Baylor SM (1997). AM-loading of fluorescent Ca^{2+} indicators into intact single fibres of frog muscle. *Biophys J* **72**, 2736–2747.

Acknowledgements

We thank Dr Knox Chandler for comments on the manuscript. This work was supported by grants from the Muscular Dystrophy Association, the US National Institutes of Health (GM 86167, EY13862), and the Pennsylvania Department of Health. The Department of Health specifically disclaims responsibility for any analyses, interpretations or conclusions.